Interfacial hydroxyl promotes the reduction of 4-Nitrophenol by Ag-based catalysts confined in dendritic mesoporous silica nanospheres

Xiao-Dan Hu,[1¶] Bing-Qian Shan,[1¶] Ran Tao,[1] Tai-Qun Yang,[1*] Kun Zhang[1,2,3*]

[1] Shanghai Key Laboratory of Green Chemistry and Chemical Processes, Laboratory of Interface and Water Science, College of Chemistry and Molecular Engineering, East China Normal University, Shanghai 200062, China;

[2] Laboratoire de chimie, Ecole Normale Supérieure de Lyon, Institut de Chimie de Lyon, Université de Lyon, 46 Allée d'italie, 69364 Lyon cedex 07, France;

[3] Shandong Provincial Key Laboratory of Chemical Energy Storage and Novel Cell Technology, School of Chemistry and Chemical Engineering, Liaocheng University, Liaocheng, 252059, Shandong, P. R. China.

¶ XDH and BQS equally contribute this research;* Correspondence: tqyang@ chem.ecnu.edu.cn (TQY); kzhang@chem.ecnu.edu.cn (K.Z.)

Abstract:

It has been widely accepted that decreasing the pH value could enhance the reactivity of 4-Nitrophenol (4-NP) reduction accompanied with the pillage of H_2, but excess hydrogen generation is wasteful and easy to lead to safety problems. Herein, we show that, contrast to previously reported results, interfacial adsorbed hydroxyl significantly promotes reduction of 4-NP using Ag-based nanoparticles (NPs) confined in dendritic mesoporous silica nanospheres (Ag@DMSNs) as a model catalyst at medium concentration of sodium hydroxide (NaOH). We provide strong evidences that adsorptive 4-NP and hydroxyl could spatially interact to form an intermediate state through p-p overlapping of O atoms at nanoscale interface of Ag NPs, which leads to electron redistribution and accelerates N=O bonds cleavage, and consequently accelerates the reduction of 4-NP. The findings of this work demonstrate that improving the catalytic performance can be holistically achieved through manipulating the weak interactions between reactant and enthetic species on the molecule level.

Introduction:

4-Aminophenol (4-AP), the reduction product of 4-NP, is a potent intermediate for the manufacture of pharmaceuticals and dyes.[1] However, without the catalyst, the hydrogenation of 4-NP to 4-AP by $NaBH_4$ is kinetically restricted due to kinetic barriers resulting from the large potential difference between 4-NP and BH_4^-.[2] In recent years, noble metal nanoparticles (MNPs) have been discovered to exhibit high catalytic activity for selective reduction of 4-NP in the presence of $NaBH_4$, such as Ag NPs,[3] Au NPs,[4] Pd NPs,[5] and Pt NPs.[6] Among these MNPs catalysts, Ag-based catalysts are distinctive (easy preparation, relatively low cost, less toxicity, high activity and good stability) and have been extensively utilized for 4-NP reduction.[7] However, it should be noted that MNPs catalysts are susceptible to suffer from aggregating due to the Van der Waals forces and high surface free energy.[8] For 4-NP reduction on Ag-based catalysts, the formation of large metal particles largely affects the catalytic activity and reusable performance. Accordingly, silver nanoparticles anchored through organic (such as polymers and DNA)[9] or inorganic (such as glasses, metal oxides and zeolites)[10] templates have been proposed to address the above issues. Among them, dendritic mesoporous silica nanospheres

(DMSNs) composed of cage-like spherical nanopores have been confirmed as a unique confinement matrix for the encapsulation of MNPs and enable their application in catalysis.[11]

The catalytic performance of MNPs catalysts strongly depends on their microstructure (catalyst composition, exposed crystal face, defect sits, adsorbed species, etc.) and reaction microenvironment (pressure, solvent, pH etc.). Although the reduction of 4-NP is intensively studied as a model reaction, the reaction mechanism is not yet fully comprehended. It is widely accepted that the reduction of 4-NP follows a multistep reduction process and the 4-hydroxylaminophenol (Hx) is a relative stable intermediate,[7c, 12] as shown in Scheme 1. Noting that the pH value could dramatically influence the reaction process (reduced by borohydride or molecular hydrogen), even change the reaction order.[13] Generally, at low pH, 4-NP is reduced by activated molecular hydrogen which gives a relative high reactivity. However, this may lead to a large amount of hydrogen overflow which was uneconomic and may cause safety problem. At high pH, the hydrolysis of $NaBH_4$ was largely inhibited and 4-NP was reduced by borohydride (BH_4^-), which was moderate but generally with a relative low reactivity.

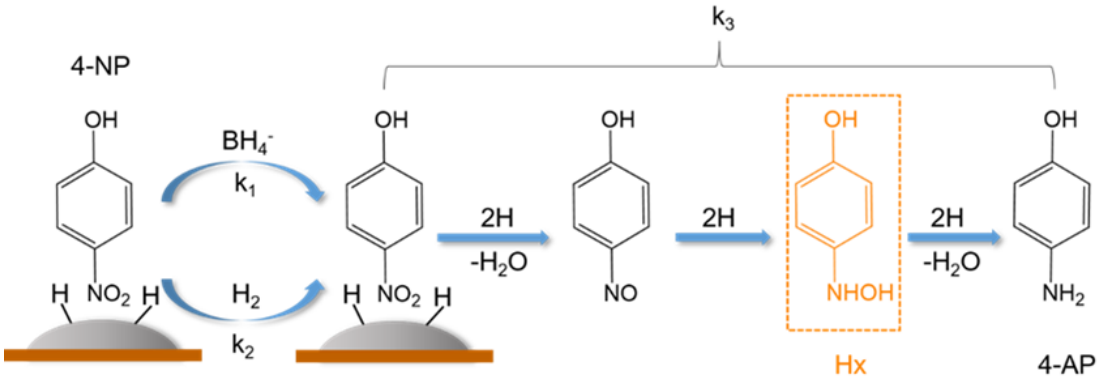

Scheme 1. Scheme illustration of 4-NP reduction following a multistep reduction process (with rate constant k_3) by adsorbed atomic hydrogen formed on Ag NPs surface using borohydride (with rate constant k_1) and molecular hydrogen (with rate constant k_2), respectively.[14]

Herein, we present a comprehensive survey of 4-NP reduction over Ag NPs confined in DMSNs via adjusting the surface microenvironment of catalyst. The experimental results demonstrated that these as-obtained Ag@DMSNs nanocomposites exhibit excellent catalytic activity for reduction of 4-NP to 4-AP under proper alkaline condition. The extraordinary activity can be explained using a mechanism involving adsorptive 4-NP and hydroxyl as the intermediate state through space interaction, while 4-NP reduction is catalyzed by the broken of N=O bonds on the Ag NPs surfaces with the intermediate state as promoter. This allows us to provide some new insights into fundamental issues concerning the molecular mechanism of heterogeneous catalytic reaction at nanoscale interfaces.

Results and discussion:

Ag-based catalysts (Ag@DMSNs) were fabricated through in-situ nanocrystal seeding-induced-growth (SIG) strategy using dendritic mesoporous silica nanospheres

(DMSNs) as a distinctive confinement matrix wherein the highly dispersed Ag NPs with narrow particle size distribution were obtained with the confinement effect of nanopores about 3 nm nested in the dendritic channels (Figure 1, a and b, synthetic details in SI). High-angle annular dark field scanning TEM (HAADF-STEM) (Figure 1c) and STEM-energy dispersive X-ray (EDX) elemental mappings (Figure 1c) further confirmed that Ag NPs were encapsulated into the pores of DMSNs. All of these results demonstrate that the ultra-small Ag NPs are successfully embedded in DMSNs.

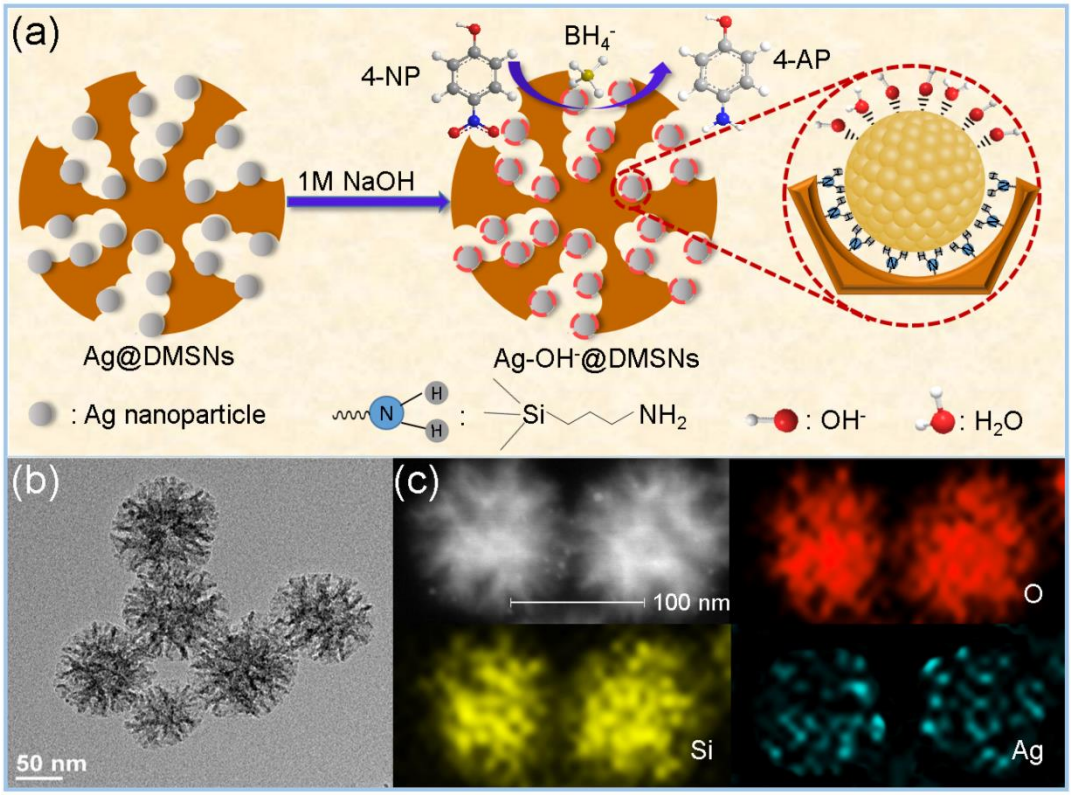

Figure 1. (a) Schematic illustration of the synthesis procedure of Ag@DMSNs. Bright-field TEM (b) and High-resolution HAADF-STEM (c) of 2.0%Ag@DMSNs and corresponding STEM EDX mappings: Si (Yellow), O (Red) and Ag (Blue), respectively.

To evaluate the size effect of Ag NPs on catalytic performance, Ag@DMSNs with different loading amounts of Ag were presented. The diffraction patterns are depicted in Figure S1a, which assigned to typical cubic phase Ag reflection peaks (JCPDS card no.04-0783) and the particle size of Ag NPs gradually increased with the increment of Ag loading amounts. The Ag NPs with size larger than 5.0 nm will be found on the external surface of DMSNs when the loading of Ag exceeding 5% (Figure S1a and Figure S2). The catalytic activity of Ag@DMSNs is size-dependent and exhibits volcano-like curve, in which the sample with the moderate loading amount (2.0%) showed the highest activity (Figure S1b).[15] Therefore, 2.0% was the best Ag loading amount and applied for further investigation.

Four typical Ag-based catalysts with same loading amount of Ag were designed, denoted as 2.0%Ag^+@DMSNs, 2.0%Ag_2O@DMSNs, 2.0%Ag@DMSNs and 2.0%Ag-OH^-@DMSNs (alkali treated), respectively. Without alkali treatment, 2.0%Ag^+@DMSNs exhibit the best catalytic activity (Figure 2a). The UV-vis spectra were

presented in Figure 2b. No distinct surface plasmon resonance (LSPR) absorption peak for 2.0%Ag^+@DMSNs was observed, which conclude that no large Ag NPs formed without reductant ($NaBH_4$). XPS spectra show that 17.2% Ag^0 was detected in 2.0%Ag^+@DMSNs which account for the excellent catalytic performance (table S1). 2.0%Ag_2O@DMSNs showed a wider characteristic peak at ~442 nm indicating the formation of Ag_2O.[16] 2.0%Ag@DMSNs and 2.0%Ag-OH^-@DMSNs exhibit the same absorption peaks at approximately 410nm (LSPR absorption), indicating identical size of Ag NPs for these two catalysts which was further verified by XRD results (Figure S3).[17] It is worth noting that the catalytic activity of Ag NPs dramatically improved after alkali treatment, surpassing most of previously reported Ag-based nanocatalysts (table S2). As shown in Figure 2a, the reaction rate of Ag NPs significantly increased from 0.55 min^{-1} (2.0%Ag@DMSNs) to 1.27 min^{-1} (2.0%Ag-OH^-@DMSNs) after alkali treatment, and even much faster than that of 2.0%Ag^+@DMSNs. To check the surface composition and the valance state of the Ag nanocatalysts before and after alkali treatment, XPS was carried out (Figure 2, c and d). The Ag 3d spectra of 2.0%Ag@DMSNs and 2.0%Ag-OH^-@DMSNs are fitted with two components accordant with the Ag^0 and Ag^+ peaks. To our surprise, the proportion of Ag^+ component was increased from 7.5% (2.0%Ag@DMSNs: 0.55 min^{-1}) to 63.7% (2.0%Ag-OH^-@DMSNs: 1.27 min^{-1}), which is close to the content (82.8 %) of Ag^+ in the sample of 2.0%Ag^+@DMSNs,[18] and the fitting results were summarized in table S1. Obviously, the valence of Ag particles affects the rate of reduction reaction, but that is not the decisive factor. To our surprise, the

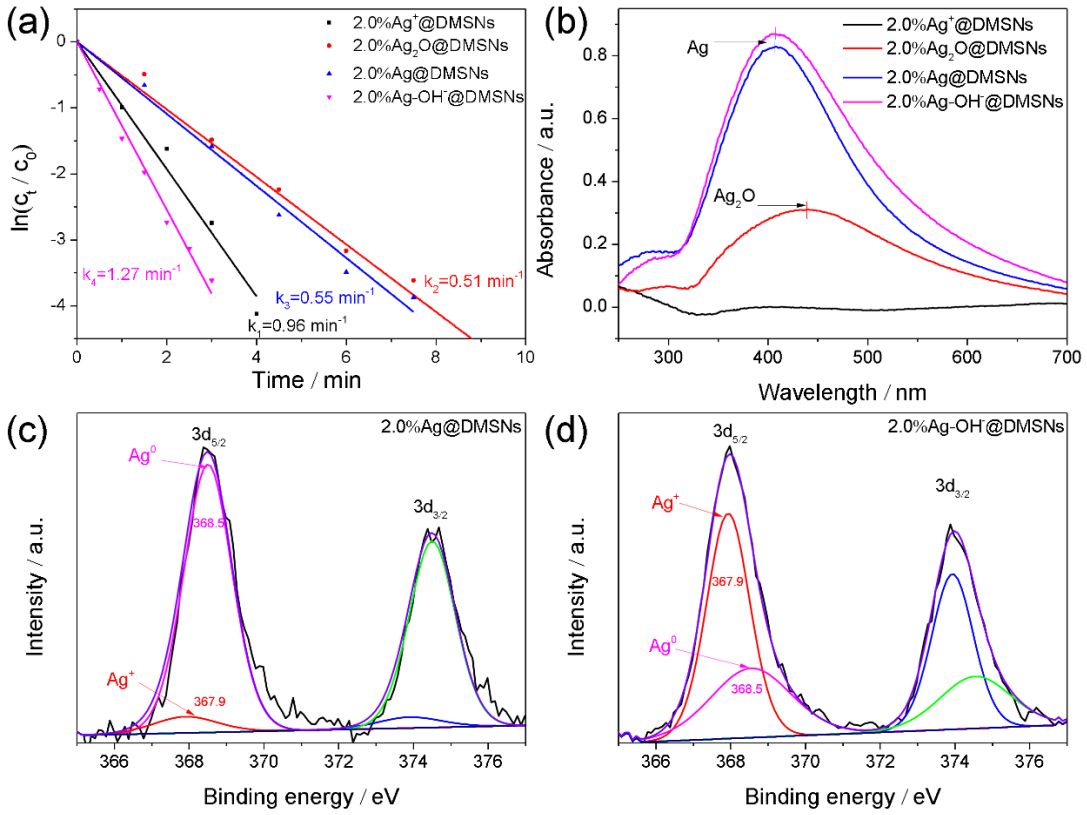

Figure 2. The catalytic activity (a) and UV-vis absorption spectra (b) of different Ag-based catalysts with same loading amount of Ag. Ag 3d XPS spectra of 2.0%Ag@DMSNs (c) and 2.0%Ag-OH^-@DMSNs (d).

preparation method of parent catalysts, especially the pre-adsorption of OH^- on the Ag NPs and the amount of adsorption ultimately determine its catalytic performance (Figure S5).

Generally, the reduction rate of 4-NP to 4-AP sharply decreases in solution at high alkalinity, which is mainly attributed to the lower hydrolysis rate of $NaBH_4$ (H_2-driven reductions, Scheme 1).[13b, 19] However, in our case, the catalytic activity was significantly enhanced for the 2.0%Ag-OH-@DMSNs as discussed above, indicating a main contribution from the hydroxyl in boosting up the conversion of 4-NP. To further verify the role of hydroxyl toward 4-NP reduction, sodium hydroxide (NaOH) solution with varied concentration is introduced to reaction system to investigate the relationship between catalytic activity and alkalinity. Unexpectedly, the reaction rate the parent catalysts of 2.0%Ag-OH^-@DMSNs with highest catalytic activity decreased with the increase of NaOH concentration (Figure 3d), and the same trend is found for catalyst of 2.0%Ag_2O@DMSNs (Figure 3c). This indicates that excessive addition of OH^- will retard the reaction, probably due to the quenching of $NaBH_4$ hydrolysis. On the contrary, with the increase of OH^- concentration, for other two catalysts of 2.0%Ag+@DMSNs and 2.0%Ag@DMSNs, the reaction rate first slightly reduces, and then raises up to maximum value, and finally reduce again (Figure 3, a and b), implying that moderate alkalinity (1M NaOH) is conductive to superior catalytic activity for Ag@DMSNs nanocomposites. Since the strong coordination interaction between OH^- ligands and surface coordinatively unsaturated Ag atoms, during the catalytic reaction, the OH^- ligand can be readily adsorbed onto the

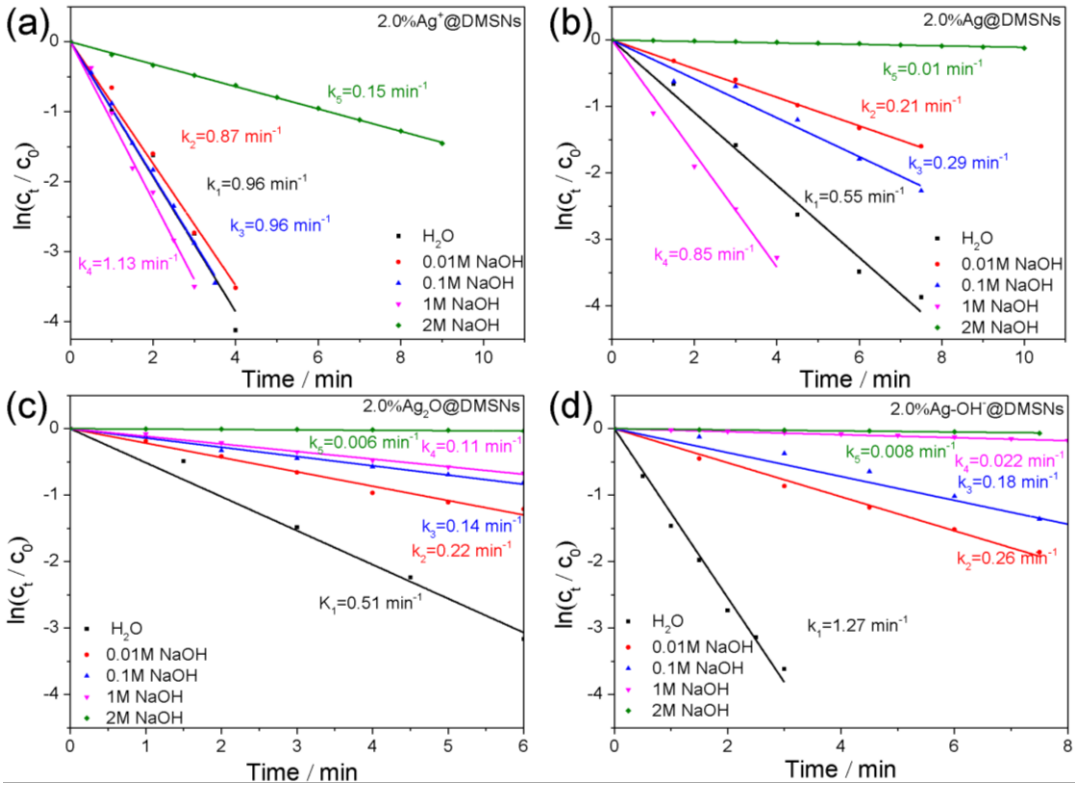

Figure 3. Plots of $\ln(C_t/C_0)$ against the reaction time of the reduction of *4*-NP over 2.0%Ag^+@DMSNs (a), 2.0%Ag@DMSNs (b), 2.0%Ag_2O@DMSNs (c) and 2.0%Ag-OH^-@DMSNs (d) with different concentrations of sodium hydroxide as solvent instead of water.

surface of Ag NPs. Indeed, the same catalyst as parent 2.0%Ag-OH-@DMSNs is formed. Obviously, the new formed interface states or species triggered by the adsorption of OH^- anions with proper amount promote the reaction rate.

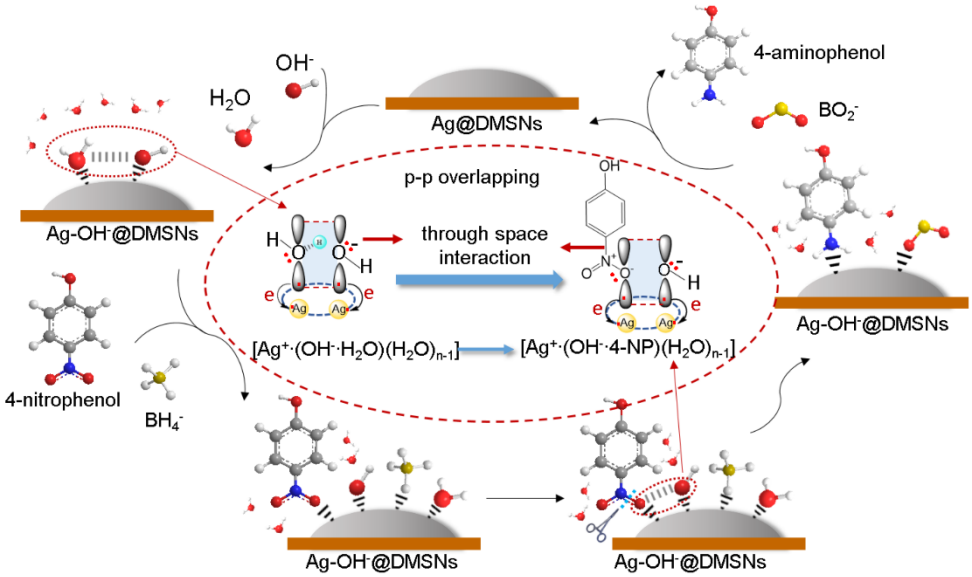

Figure 4. Proposed mechanism for the 4-NP reduction by $NaBH_4$ in the presence of a 2.0%Ag-OH^-@DMSNs catalyst.

To provide an insight behind the outstanding catalytic activity generated by the Ag NPs embedded in the DMSNs support with presence of interfacial hydroxyl, a coherent catalytic mechanism is suggested as shown in Figure 4. In this model, the presence of hydroxyl facilitates strong H-bond interactions between the water and hydroxyl, forming a new hydrated hydroxide intermediate $[Ag^+\cdot(OH^-\cdot H_2O)(H_2O)_{n-1}]$ (in red circle).[20] The resulting hydrated hydroxide complexes are weakly adsorbed onto the metal core surface due to the coordination effect between O and coordinatively unsaturated Ag atoms. Recently, these intermediate states were captured by steady and ultra-fast transient absorption spectrum, which is formed through space interaction of p orbitals of paired O atoms in the hydrated hydroxide complexes; and upon the photoexcitation, the bright tunable photoluminescence (PL) emissions were observed with character of π→π* transition. [20a, 20c, 21] The absorption and emission feature confirms the presence of these intermediate states when hydroxyl groups are present (Figure 5, a and b, blue line). During the catalytic conversion of 4-NP to 4-AP, both reactants 4-NP and BH_4^- first migrated to the pores and then were adsorbed around the active Ag nanocatalysts according to the Langmuir−Hinshelwood approach.[22] Simultaneously, the adjacent O atoms between 4-NP and hydroxyl locally interact with each other which was compete with the preformed hydrated hydroxide intermediate to form new intermediate state $[Ag^+\cdot(OH^-\cdot 4\text{-NP})(H_2O)_{n-1}]$ by the overlapping of p-orbitals with high-energy lone-pair electrons. The structural discrepancy of two intermediate states implies the change of interaction strength between two O···O atoms and determines the overlapping degree of two p orbitals of O atoms, as evidenced by the excitation and photoemission spectra (Figure 5, a and b, green line). Upon the addition of 4-NP reactant, the excitation at ca. 300 nm and emission at ca. 500 nm was significantly intensified. In the new formed

intermediate state [$Ag^{+}\cdot(OH^{-}\cdot$4-NP$)(H_2O)_{n-1}$], electrons are largely delocalized between nitro and hydroxyl due to the overlapping of p-orbitals between N and O atoms. The electron communication between nitro and hydroxyl could form a new molecular energy level and lower the bond energy of N=O (or the activation of N=O bond) which is beneficial to promote the breaking of N=O bond in 4-NP molecule to proceed the hydrogenation reaction. We believe that the Ag nanoparticles are not only useful for adsorbing reactants, but can also stabilize the intermediate states structure by weak interactions (ion-dipole interaction).[23]

To convince the switch between these two presented intermediate states, the photoluminescence spectra (PL) were elaborately analyzed. As shown in Figure 5a and 5b, no obvious PL signal was observed for catalysts without interfacial hydroxyl (black and red line). However, when these non-luminescent Ag@DMSNs nanocomposites were dispersed into the mixed H_2O/NaOH or 4-NP/NaOH solution, distinct luminescence properties were observed (blue and green line). Intriguingly, the variation of relative intensity between the excitation peaks at ~290, 330nm were observed which implying the switch of intermediate state from [$Ag^{+}\cdot(OH^{-}\cdot H_2O)(H_2O)_{n-1}$] to [$Ag^{+}\cdot(OH^{-}\cdot$4-NP$)(H_2O)_{n-1}$]. For the Ag@DMSNs nanocomposites containing interfacial hydroxyl (2.0%Ag_2O@DMSNs and 2.0%Ag-OH^{-}@DMSNs), similar PL properties were observed (Figure 5, c and d), which further evidenced the important role of hydroxyl. In a word, the luminescence properties are highly dependent on the presence of interfacial hydroxyl on the confined nanointerface of Ag NPs, which could interact with adsorbed reactants to form an intermediate state and change the reaction route and reduce the activation energy ($\boldsymbol{E}_a$) as schemed in Figure 4, finally, enhance reduction reactivity of 4-NP.

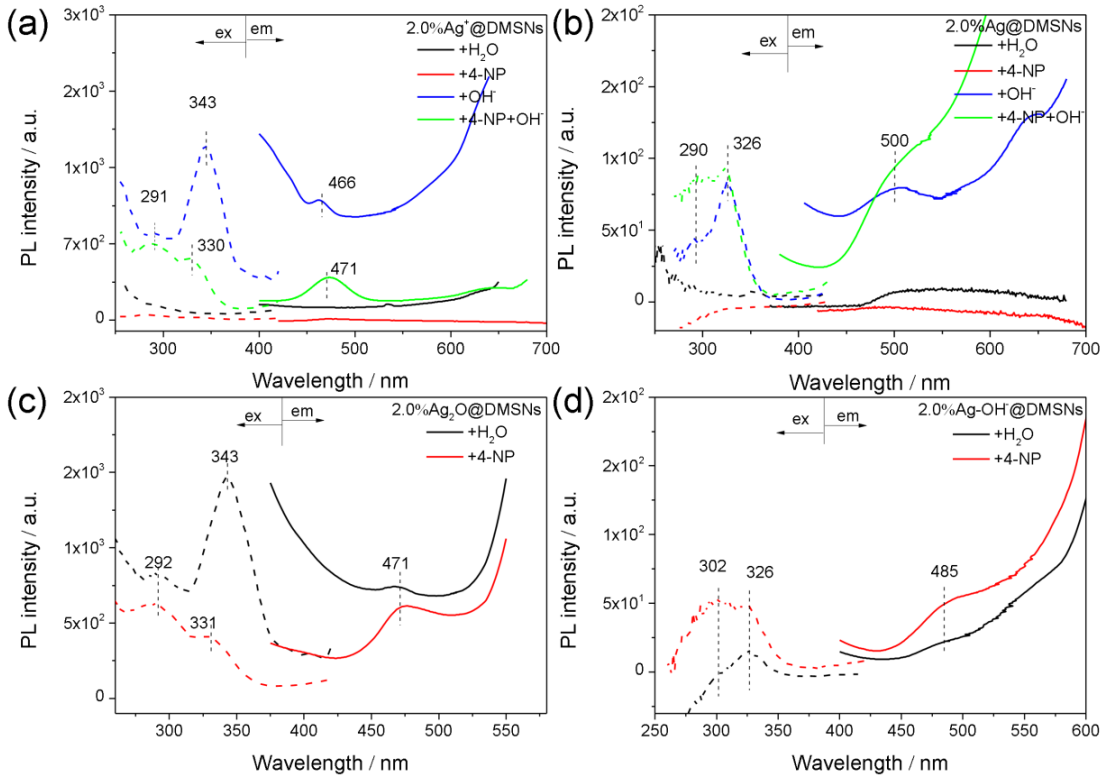

Figure 5. Excitation (dot line) and emission spectra (solid line) of 2.0%Ag^{+}@DMSNs (a), 2.0%Ag@DMSNs (b), 2.0%Ag_2O@DMSNs (c), 2.0%Ag-OH^{-}@DMSNs (d).

Conclusions:

In summary, we have provided incontrovertible evidence that hydroxyl introduced to the reaction system could enhance the catalytic activity toward the reduction of 4-NP by $NaBH_4$. A new intermediate state, resulting from the strong overlapping of p orbitals between 4-NP and hydroxyl through space interactions, is identified as a promoter to activate the N=O bond. The proposed intermediate state model clearly answers the excellent catalytic activity on the 4-NP reduction which was further evidenced by the PL spectra. This hydroxyl promoted hydrogenation could largely improve the hydrogen utilization and this significant conceptual advance provides completely new mechanic insights for the understanding of selective hydrogenation reactions and is guide to design to new heterogeneous catalysts by molecularly manipulating the surface microenvironment at the nanoscale interface.[24]

Acknowledgments: This research was funded by the NSFC (21872053 and 21573074), the Science and Technology Commission of Shanghai Municipality (19520711400), the CAS key laboratory of Low-Coal Conversion Science & Engineering (KLLCCSE-201702), and the JORISS program, the Postdoctoral Science Foundation of China (2018M640360). K.Z. thanks ENS de Lyon for a temporary position as an invited professor in France.

Reference

1. (a) Du, Y.; Chen, H.; Chen, R.; Xu, N., Synthesis of p-aminophenol from p-nitrophenol over nano-sized nickel catalysts. *Appl. Catal. A-Gen.* **2004,** *277* (1-2), 259-264; (b) Fu, Y.; Huang, T.; Jia, B.; Zhu, J.; Wang, X., Reduction of nitrophenols to aminophenols under concerted catalysis by Au/g-C3N4 contact system. *Appl. Catal. B.* **2017,** *202*, 430-437; (c) Vaidya, M. J.; Kulkarni, S. M.; Chaudhari, R. V., Synthesis of p-Aminophenol by Catalytic Hydrogenation of p-Nitrophenol. *Org. Proc. Res. Dev.* **2003,** *7*, 202−208.

2. (a) Baruah, B.; Gabriel, G. J.; Akbashev, M. J.; Booher, M. E., Facile synthesis of silver nanoparticles stabilized by cationic polynorbornenes and their catalytic activity in 4-nitrophenol reduction. *Langmuir* **2013,** *29* (13), 4225-34; (b) Gangula, A.; Podila, R.; M, R.; Karanam, L.; Janardhana, C.; Rao, A. M., Catalytic reduction of 4-nitrophenol using biogenic gold and silver nanoparticles derived from Breynia rhamnoides. *Langmuir* **2011,** *27* (24), 15268-74.

3. Yan, Z.; Fu, L.; Zuo, X.; Yang, H., Green assembly of stable and uniform silver nanoparticles on 2D silica nanosheets for catalytic reduction of 4-nitrophenol. *Appl. Catal. B.* **2018,** *226*, 23-30.

4. Neal, R. D.; Hughes, R. A.; Sapkota, P.; Ptasinska, S.; Neretina, S., Effect of Nanoparticle Ligands on 4-Nitrophenol Reduction: Reaction Rate, Induction Time, and Ligand Desorption. *ACS Catal.* **2020,** *10* (17), 10040-10050.

5. Huang, L.; Zou, J.; Ye, J.-Y.; Zhou, Z.-Y.; Lin, Z.; Kang, X.; Jain, P. K.; Chen, S., Synergy between Plasmonic and Electrocatalytic Activation of Methanol Oxidation on Palladium-Silver Alloy Nanotubes. *Angew. Chem. Int. Ed.* **2019,** *58* (26), 8794-8798.

6. Liu, J.; He, K.; Wu, W.; Song, T. B.; Kanatzidis, M. G., In Situ Synthesis of Highly Dispersed and Ultrafine Metal Nanoparticles from Chalcogels. *J. Am. Chem. Soc.* **2017,** *139* (8), 2900-2903.

7. (a) Xu, P.; Liang, X.; Chen, N.; Tang, J.; Shao, W.; Gao, Q.; Teng, Z., Magnetic separable chitosan microcapsules decorated with silver nanoparticles for catalytic reduction of 4-nitrophenol. *J. Colloid Interface Sci.* **2017,** *507*, 353-359; (b) Liu, S.; Qi, Y.; Cui, L.; Dai, Q.; Zeng, S.; Bai, C., Controllable

synthesis of silver anchored N-doped yolk-shell carbon@mSiO2 spheres and their application for the catalytic reduction of 4-nitrophenol. *Appl. Surf. Sci.* **2019,** *493*, 1013-1020; (c) Liao, G.; Gong, Y.; Zhong, L.; Fang, J.; Zhang, L.; Xu, Z.; Gao, H.; Fang, B., Unlocking the door to highly efficient Ag-based nanoparticles catalysts for NaBH4-assisted nitrophenol reduction. *Nano Res.* **2019,** *12* (10), 2407-2436.

8. (a) Pandiarajan, J.; Krishnan, M., Properties, synthesis and toxicity of silver nanoparticles. *Environ. Chem. Lett.* **2017,** *15* (3), 387-397; (b) Evanoff, D. D., Jr.; Chumanov, G., Synthesis and optical properties of silver nanoparticles and arrays. *Chemphyschem : a European journal of chemical physics and physical chemistry* **2005,** *6* (7), 1221-31; (c) Chi, Y.; Yuan, Q.; Li, Y.; Tu, J.; Zhao, L.; Li, N.; Li, X., Synthesis of Fe3O4@SiO2-Ag magnetic nanocomposite based on small-sized and highly dispersed silver nanoparticles for catalytic reduction of 4-nitrophenol. *J. Colloid Interface Sci.* **2012,** *383* (1), 96-102.

9. (a) Lu, S.; Yu, J.; Cheng, Y.; Wang, Q.; Barras, A.; Xu, W.; Szunerits, S.; Cornu, D.; Boukherroub, R., Preparation of silver nanoparticles/polydopamine functionalized polyacrylonitrile fiber paper and its catalytic activity for the reduction 4-nitrophenol. *Appl. Surf. Sci.* **2017,** *411*, 163-169; (b) Zhou, W.; Fang, Y.; Ren, J.; Dong, S., DNA-templated silver and silver-based bimetallic clusters with remarkable and sequence-related catalytic activity toward 4-nitrophenol reduction. *Chem. Commun.* **2019,** *55* (3), 373-376.

10. (a) Li, W.; Ge, X.; Zhang, H.; Ding, Q.; Ding, H.; Zhang, Y.; Wang, G.; Zhang, H.; Zhao, H., Hollow mesoporous SiO2 sphere nanoarchitectures with encapsulated silver nanoparticles for catalytic reduction of 4-nitrophenol. *Inorg. Chem. Front.* **2016,** *3*, 663–670; (b) Deshmukh, S. P.; Dhokale, R. K.; Yadav, H. M.; Achary, S. N.; Delekar, S. D., Titania–supported silver nanoparticles: An efficient and reusable catalyst for reduction of 4-nitrophenol. *Appl. Surf. Sci.* **2013,** *273*, 676-683; (c) Chiou, J. R.; Lai, B. H.; Hsu, K. C.; Chen, D. H., One-pot green synthesis of silver/iron oxide composite nanoparticles for 4-nitrophenol reduction. *J. Hazard. Mater.* **2013,** *248-249*, 394-400; (d) Manno, R.; Sebastian, V.; Irusta, S.; Mallada, R.; Santamaria, J., Ultra-Small Silver Nanoparticles Immobilized in Mesoporous SBA-15. Microwave-Assisted Synthesis and Catalytic Activity in the 4-Nitrophenol Reduction. *Catalysis Today* **2020**; (e) Simo, A.; Polte, J.; Pfander, N.; Vainio, U.; Emmerling, F.; Rademann, K., Formation mechanism of silver nanoparticles stabilized in glassy matrices. *Journal of the American Chemical Society* **2012,** *134* (45), 18824-33.

11. (a) Yang, T.-Q.; Ning, T.-Y.; Peng, B.; Shan, B.-Q.; Zong, Y.-X.; Hao, P.; Yuan, E.-H.; Chen, Q.-M.; Zhang, K., Interfacial electron transfer promotes photo-catalytic reduction of 4-nitrophenol by Au/Ag2O nanoparticles confined in dendritic mesoporous silica nanospheres. *Catal. Sci. & Technol.* **2019,** *9* (20), 5786-5792; (b) Yu, Y. J.; Xing, J. L.; Pang, J. L.; Jiang, S. H.; Lam, K. F.; Yang, T. Q.; Xue, Q. S.; Zhang, K.; Wu, P., Facile synthesis of size controllable dendritic mesoporous silica nanoparticles. *ACS Appl. Mater. Interface* **2014,** *6* (24), 22655-65; (c) Zhang, K.; Xu, L. L.; Jiang, J. G.; Calin, N.; Lam, K. F.; Zhang, S. J.; Wu, H. H.; Wu, G. D.; Albela, B.; Bonneviot, L.; Wu, P., Facile large-scale synthesis of monodisperse mesoporous silica nanospheres with tunable pore structure. *J. Am. Chem. Soc.* **2013,** *135* (7), 2427-30; (d) Liu, P.-C.; Yu, Y.-J.; Peng, B.; Ma, S.-Y.; Ning, T.-Y.; Shan, B.-Q.; Yang, T.-Q.; Xue, Q.-S.; Zhang, K.; Wu, P., A dual-templating strategy for the scale-up synthesis of dendritic mesoporous silica nanospheres. *Green Chem.* **2017,** *19* (23), 5575-5581; (e) Hao, P.; Peng, B.; Shan, B.-Q.; Yang, T.-Q.; Zhang, K., Comprehensive understanding of the synthesis and formation mechanism of dendritic mesoporous silica nanospheres. *Nanoscale Adv.* **2020,** *2* (5), 1792-1810.

12. Corma, A.; Concepción, P.; Serna, P., A Different Reaction Pathway for the Reduction of Aromatic Nitro Compounds on Gold Catalysts. *Angew.Chem. Int. Ed.* **2007,** *119* (38), 7404-7407.

13. (a) WeiXie; Grzeschik, R.; Schlücker, S., Metal Nanoparticle-Catalyzed Reduction Using Borohydridein Aqueous Media:A Kinetic Analysis of the Surface Reaction by Microfluidic SERS. *Angew.Chem. Int. Ed.* **2016,** *55*, 13729 –13733; (b) Grzeschik, R.; Schäfer, D.; Holtum, T.; Sebastian Küpper; Hoffmann, A.; Schlücker, S., On the Overlooked Critical Role of the pH Value on the Kinetics of the 4‐Nitrophenol NaBH4‐Reduction Catalyzed by Noble-Metal Nanoparticles (Pt, Pd, and Au). *J. Phys. Chem. C* **2020,** *124*, 2939−2944.

14. Liao, G.; Gong, Y.; Zhong, L.; Fang, J.; Zhang, L.; Xu, Z.; Gao, H.; Fang, B., Unlocking the door to highly efficient Ag-based nanoparticles catalysts for NaBH4-assisted nitrophenol reduction. *Nano Research* **2019,** *12* (10), 2407-2436.

15. (a) Fenger, R.; Fertitta, E.; Kirmse, H.; Thunemann, A. F.; Rademann, K., Size dependent catalysis with CTAB-stabilized gold nanoparticles. *Phys. Chem. Chem. Phys.* **2012,** *14* (26), 9343-9349; (b) Kon, K.; Hakim Siddiki, S. M. A.; Shimizu, K.-i., Size- and support-dependent Pt nanocluster catalysis for oxidant-free dehydrogenation of alcohols. *J. Catal.* **2013,** *304*, 63-71.

16. Wang, X.; Li, S.; Yu, H.; Yu, J.; Liu, S., Ag2O as a new visible-light photocatalyst: self-stability and high photocatalytic activity. *Chem. Eur. J.* **2011,** *17* (28), 7777-7780.

17. (a) Pu, F.; Huang, Y.; Yang, Z.; Qiu, H.; Ren, J., Nucleotide-Based Assemblies for Green Synthesis of Silver Nanoparticles with Controlled Localized Surface Plasmon Resonances and Their Applications. *ACS Appl. Mater. Interface* **2018,** *10* (12), 9929-9937; (b) Jung, H.-Y.; Yeo, I.-S.; Kim, T.-U.; Ki, H.-C.; Gu, H.-B., Surface plasmon resonance effect of silver nanoparticles on a TiO 2 electrode for dye-sensitized solar cells. *Appl. Surf. Sci.* **2018,** *432*, 266-271.

18. (a) Budi, C. S.; Deka, J. R.; Saikia, D.; Kao, H. M.; Yang, Y. C., Ultrafine bimetallic Ag-doped Ni nanoparticles embedded in cage-type mesoporous silica SBA-16 as superior catalysts for conversion of toxic nitroaromatic compounds. *J. Hazard. Mater.* **2019,** *384*, 121270; (b) Kumar, M.; Deka, S., Multiply twinned AgNi alloy nanoparticles as highly active catalyst for multiple reduction and degradation reactions. *ACS Appl. Mater. Interface* **2014,** *6* (18), 16071-81.

19. (a) Lin, F.-h.; Doong, R.-a., Highly efficient reduction of 4-nitrophenol by heterostructured gold-magnetite nanocatalysts. *Appl. Catal. A-Gen.* **2014,** *486*, 32-41; (b) Churikov, A. V.; Gamayunova, I. M.; Zapsis, K. V.; Churikov, M. A.; Ivanishchev, A. V., Influence of temperature and alkalinity on the hydrolysis rate of borohydride ions in aqueous solution. *Int. J. Hydrogen Energy* **2012,** *37* (1), 335-344; (c) Kim, J.-H.; Lee, H.; Han, S.-C.; Kim, H.-S.; Song, M.-S.; Lee, J.-Y., Production of hydrogen from sodium borohydride in alkaline solution: development of catalyst with high performance. *Int. J. Hydrogen Energy* **2004,** *29*, 263–267.

20. (a) Yang, T.; Shan, B.; Huang, F.; Yang, S.; Peng, B.; Yuan, E.; Wu, P.; Zhang, K., P band intermediate state (PBIS) tailors photoluminescence emission at confined nanoscale interface. *Commun. Chem.* **2019,** *2* (1); (b) Yang, T.-Q.; Peng, B.; Zhou, J.-F.; Shan, B.-Q.; Zhang, K., Hydrogen-Bonded Water Clusters Confined in Nanocavity as Bright Color Emitters. *ChemRxiv* **2020**; (c) Hu, X.-D.; Yang, T.-Q.; Shan, B.-Q.; Peng, B.; Zhang, K., Topological excitation of singly hydrated hydroxide complex in confined sub-nanospace for bright color emission and heterogeneous catalysis. *ChemRxiv* **2020**.

21. (a) Hoffmann, R., Interaction of Orbitals through Space and through Bonds. *Acc. Chem. Res.* **1971,** *4*, 1-9; (b) Takahashi, M.; Ogino, R.; Udagawa, Y., An electron momentum spectroscopy study of p orbitals of norbornadiene and 1,4-cyclohexadiene: evidence for through-space and through-bond interactions. *Chem. Phys. Letts.* **1998,** *288*, 714–8; (c) Yang, T. Q.; Peng, B.; Shan, B. Q.; Zong, Y. X.; Jiang, J. G.; Wu, P.; Zhang, K., Origin of the Photoluminescence of Metal Nanoclusters: From Metal-Centered Emission to Ligand-Centered Emission. *Nanomaterials (Basel)* **2020,** *10* (2).

22. (a) Wunder, S.; Polzer, F.; Lu, Y.; Mei, Y.; Ballauff, M., Kinetic Analysis of Catalytic Reduction of 4-Nitrophenol by Metallic Nanoparticles Immobilized in Spherical Polyelectrolyte Brushes. *J. Phys. Chem. C* **2010,** *114*, 8814–8820; (b) Antonels, N. C.; Meijboom, R., Preparation of well-defined dendrimer encapsulated ruthenium nanoparticles and their evaluation in the reduction of 4-nitrophenol according to the Langmuir-Hinshelwood approach. *Langmuir* **2013,** *29* (44), 13433-42; (c) Thawarkar, S. R.; Thombare, B.; Munde, B. S.; Khupse, N. D., Kinetic investigation for the catalytic reduction of nitrophenol using ionic liquid stabilized gold nanoparticles. *RSC Adv.* **2018,** *8* (67), 38384-38390.

23. (a) Collins, K. D.; Neilson, G. W.; Enderby, J. E., Ions in water: characterizing the forces that control chemical processes and biological structure. *Biophys. Chem.* **2007,** *128* (2-3), 95-104; (b) Teychené, J.; Balmann, H. R.-d.; Maron, L.; Galier, S., Investigation of ions hydration using molecular modeling. *Journal of Molecular Liquids* **2019,** *294*.

24. (a) Luneau, M.; Lim, J. S.; Patel, D. A.; Sykes, E. C. H.; Friend, C. M.; Sautet, P., Guidelines to Achieving High Selectivity for the Hydrogenation of alpha,beta-Unsaturated Aldehydes with Bimetallic and Dilute Alloy Catalysts: A Review. *Chem. Rev.* **2020**; (b) Ren, X.; Guo, M.; Li, H.; Li, C.; Yu, L.; Liu, J.; Yang, Q., Microenvironment Engineering of Ruthenium Nanoparticles Incorporated into Silica Nanoreactors for Enhanced Hydrogenations. *Angew. Chem. Int. Ed.* **2019,** *58* (41), 14483-14488.